

Lattice Deduction Transformers

Liam Davis
Amherst College
ljdavis27@amherst.edu

Leopold Haller
Axiom
leo@axiommath.ai

Alberto Alfarano
Axiom
alberto@axiommath.ai

Mark Santolucito
Barnard College, Columbia University
msantolu@barnard.edu

Abstract

We introduce the Lattice Deduction Transformer (LDT), a recurrent transformer that approximates logically sound deduction by projecting its latent state through a lattice between forward passes. We train on-policy in a process that mirrors deduction in a search-based constraint solver and supervise training via a domain-agnostic, abstract-interpretation-based approximation of the set of solution candidates. An 800K-parameter LDT achieves 100% accuracy on Sudoku-Extreme and Snowflake Sudoku, at a fraction of the training cost of prior small recurrent reasoners, while remaining empirically sound: the model returns a correct answer or abstains. A 1.8M-parameter variant reaches 99.9% accuracy on Maze-Hard. Frontier LLMs score 0% on all three benchmarks.

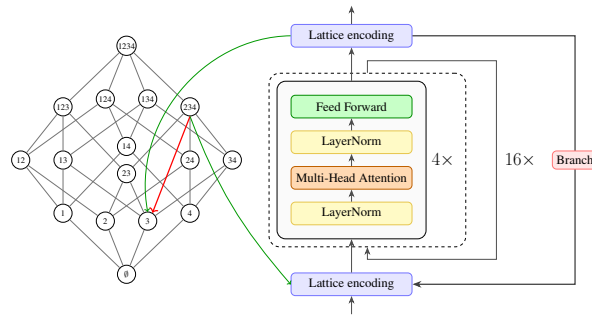


Figure 1: The Lattice Deduction Transformer (LDT) performs sound deduction on a lattice using a recurrent transformer which is alternated with search via stochastic branching.

1 Introduction

Reasoning in large language models has become largely synonymous with the chain-of-thought paradigm [1] and its test-time-compute extensions [2, 3], in which the model generates intermediate reasoning tokens before producing a final answer. In contrast, automated logical reasoning procedures operate in close analogy to discrete diffusion models [4], by iterative refinement of a partial information state. In diffusion, information is partial in the sense that some tokens are masked; refinement proceeds by progressively unmasking them. We can then view logical solvers as a special case of discrete diffusion procedures that aim to recover an element of a uniform target distribution over valid solutions, in contrast to the broader, non-uniform distributions over plausible outputs more commonly studied in the diffusion literature. It is then natural to ask whether techniques developed in the automated-reasoning literature transfer to diffusion-style algorithms, and conversely.

We consider reasoning from the perspective of *abstract interpretation* [5, 6], which models information states as elements of a lattice with a top element \top representing no information (every solution still possible) and a bottom element \perp representing inconsistency (no solution remains). Deduction is a process that descends from \top toward more informative states; a state that collapses to \perp signals that no valid solution remains. The procedure is sound by design but incomplete: a deduction step may fail to derive a true fact, but never derives a false one.

Concretely, we use a recurrent transformer whose latent state is projected to and from a lattice representation between forward passes; we call this the Lattice Deduction Transformer (LDT). The interpretability of the abstract domain lets us leverage symbolic search processes at both training and inference time. On hard problems with logical structure, LDT exceeds comparable reasoning transformers with smaller models and less training. On some domains it further achieves empirical soundness given a sufficient training budget: the search either returns a correct answer or abstains; it is never incorrect.

We make four contributions. First, an architecture that projects a recurrent transformer’s latent state onto an abstract lattice at every iteration, turning each forward pass into a sound deduction step. Second, an on-policy training procedure where lattice states evolve under the model’s own forward pass, keeping training states in-distribution with search states encountered during inference. Third, the *alpha operator*, which aggregates the valid solutions still consistent with the current lattice state. This places our training in a regime we are not aware of in prior work: on-policy yet still supervised by a domain-agnostic, state-dependent target. Fourth, an experimental characterization of the train/test compute trade-off in learned sound inference, showing that additional training shortens inference search by orders of magnitude.

The rest of the paper is organized as follows: Section 2 reviews related work. Section 3 provides relevant background on abstract interpretation and lattice structures. Section 4 details the architecture, training and inference of the Lattice Deduction Transformer. Section 5 provides an evaluation of the Lattice Deduction Transformer against comparable reasoning transformers and frontier LLMs. Finally, we conclude and discuss future directions in section 6.

2 Related Work

Our approach draws from research on small recurrent models that outperform far larger ones on hard reasoning problems. Adaptive Computation Time [7] introduced variable-iteration neural computation for recurrent networks, later adapted to transformers by Universal Transformers [8]. The Hierarchical Reasoning Model [9] uses a dual-loop recurrent architecture, and the Tiny Recursive Model [10] shows that a 2-layer network with recursion can outperform it with a smaller model. We build directly on Sotaku [11], a recurrent transformer specialized for Sudoku.

LDT can also be characterized as a neuro-symbolic method, combining a neural network with the lattice representation that search-based constraint solvers use to track partial information. SATNet [12] and Learning Modulo Theories [13] embed MAX-SAT and SMT solvers as network layers, preserving a hard neural/symbolic boundary. Closer to our setting, machine learning has been applied throughout the abstract-interpretation pipeline: Neural Abstract Interpretation [14] trains sound differentiable abstract transformers, LAIT [15] learns a neural policy that prunes redundant constraints, and SAIL [16] synthesizes sound transformers via LLMs with SMT validation. Earlier work targets the control loop instead, selecting among sound transformers via RL [17] or learning widening thresholds [18].

D3PM [4], the discrete-diffusion generalization of masked language modeling [19], iteratively commits information about partially-masked sequences; we recast this process as a fixed-point computation over a lattice. D3PM in fact admits an arbitrary token-transition matrix Q , which can be instantiated over tokens that themselves form a lattice – closely related in spirit to our setup, though we do not develop our method as a diffusion procedure. Several recent diffusion variants push in this direction. For example, ReMDM [20] reintroduces backtracking by allowing already-generated tokens to be remasked at inference time, Prime [21] relaxes the masked/unmasked dichotomy by letting tokens occupy intermediate states between \top and a concrete value, and HDLM [22] organizes the vocabulary into a refinement hierarchy whose forward process abstracts upward and reverse process refines downward. Each can be read as moving along a particular partial-information ordering; in our framing, that ordering is the lattice.

3 Abstract Interpretation

Abstract interpretation, introduced by Cousot and Cousot [5, 6], is a framework for sound approximate reasoning over systems where exact reasoning is computationally infeasible. Originally developed for program analysis, it replaces costly computation over a concrete domain C with efficient computation over an abstract domain A , while guaranteeing *soundness*: any property established in the abstract holds in the concrete.

Soundness comes at a price: a reasoner over A may fail to derive a true fact even when one is provable in C , a loss of *completeness*. In finite domains, completeness can be restored via search procedures. Propositional satisfiability algorithms such as DPLL [23, 24], CDCL [25], and Stålmarck’s procedure [26, 27] can be cast as sophisticated search-based refinement operators on an abstract domain [28, 29].

In the canonical setting, the C and A are both lattices, with the order encoding *precision* (lower elements are more informative; \top the least informative and \perp the most informative, often denoting inconsistency or impossibility). The two domains are linked by an *abstraction* function $\alpha : C \rightarrow A$ and a *concretization* function $\gamma : A \rightarrow C$, which form an adjoint pair (a *Galois connection*). This adjoint condition ensures that properties proved over A hold over C . We defer more in-depth formal exposition to a self-contained mini-tutorial in Appendix A. To illustrate, consider Sudoku puzzles: A solved puzzle is a function $g : \{1, \dots, 9\}^2 \rightarrow \{1, \dots, 9\}$ assigning a digit to each (row, column) pair. To reason about a partially solved puzzle, we want a representation that captures uncertainty about which complete grid is correct. A natural choice is the *powerset lattice* $C = 2^G$ over the set G of all complete grids: an element of C is the set of grids still considered viable given what we know so far. We order C by inclusion: smaller sets are more precise; $\top = G$ asserts no information, and $\perp = \emptyset$ records that the puzzle is unsolvable.

A natural choice of abstract domain for Sudoku is to associate with each cell the digits still considered viable, collapsing all inter-cell correlations. We call this abstract domain the *grid powerset lattice*: $A = (\{1, \dots, 9\}^2 \rightarrow 2^{\{1, \dots, 9\}})$, ordered pointwise so that $a' \sqsubseteq a$ iff $a'(c) \subseteq a(c)$ for every cell c . \top assigns every cell the full digit set, and \perp is reached when any cell’s candidate set becomes empty. Sudoku rules become sound abstract deduction operators on A : each step removes candidates without ruling out a valid solution. Naked singles and hidden singles are two simple examples of such operators. When the deduction operator is itself learned, this becomes a tradeoff between train-time compute and test-time search, which we characterize empirically in Section 5.1 (Figure 3a).

4 Methodology

We focus on problems whose solutions can be expressed as fixed-length token strings over a vocabulary V , so the solution space is $S = \{1, \dots, k\} \rightarrow V$. For an instance $p \in P$, let $\|p\| \subseteq S$ denote the set of valid solutions; we do not assume access to a closed-form description of $\|p\|$, only that samples from $\|p\|$ are available for each training instance.

Following abstract interpretation, we take the concrete domain to be the powerset lattice $C = \mathcal{P}(S)$ and the abstract domain to be $A = \{1, \dots, k\} \rightarrow \mathcal{P}(V)$, where each $a \in A$ records the still-viable candidates at every position. We order A pointwise by inclusion: $a \sqsubseteq b$ iff $a(i) \subseteq b(i)$ for every i , with meet and join defined pointwise as $(a \sqcap b)(i) = a(i) \cap b(i)$ and $(a \sqcup b)(i) = a(i) \cup b(i)$. The two domains are linked by an abstraction function $\alpha : C \rightarrow A$ with $\alpha(S')(i) = \{s(i) \mid s \in S'\}$ and a concretization function $\gamma : A \rightarrow C$ with $\gamma(a) = \{s \in S \mid \forall i. s(i) \in a(i)\}$, which together form a Galois connection. The most precise sound deduction operator on A for instance p is given by

$$ded_p(a) = \alpha(\gamma(a) \cap \|p\|).$$

Informally, ded_p refines a to keep only the candidates that survive in at least one valid solution. Our goal is to train a transformer to approximate ded_p from solution samples, without ever computing $\|p\|$ explicitly. Architecturally, we encode the lattice structure as a tensor and use input and output projections between the abstract domain and the transformer’s latent space. Algorithmically, we use the same iterative search process at training and inference time, which we found critical for keeping the transformer in-distribution at inference.

4.1 Architecture

For grid-structured problems such as Sudoku, the position indices $\{1, \dots, k\}$ identify cells of a 2D grid (e.g., $k = 81$ for 9×9 Sudoku), and the abstract domain A assigns a candidate set from $\mathcal{P}(V)$ to each cell. We refer to this instantiation as the *grid powerset lattice*.

Lattice encoding We represent the grid powerset lattice as a multi-hot encoding: $|V|$ binary sigmoids per cell (so $9 \times 9 \times 9 = 729$ sigmoids for 9×9 Sudoku; see Figure 2). Each sigmoid encodes the confidence that its candidate is still alive, and deduction corresponds to pushing sigmoids toward 0 until each cell has a single survivor. Solutions y are one-hot (one bit alive per cell), and the abstraction α over a set of solutions reduces to a bit-level OR. For variable-topology puzzles where not every grid position is part of every instance, an additional read-only mask per cell marks which positions are in-puzzle. We use this for Snowflake Sudoku in Section 5.2.

We give \perp a dual representation. The first is implicit in the candidate encoding: a cell with an empty candidate set is the natural representation of \perp in the powerset lattice. The second is an explicit binary sigmoid attached to a distinguished CLS token, which we train to fire on any unsatisfiable state. At search time, deduction tightens the lattice state forward, and we treat either an empty cell or a CLS sigmoid above θ_{CLS} as a conflict that triggers backtracking. Carrying separate representations lets us train the two heads with different losses, discussed below.

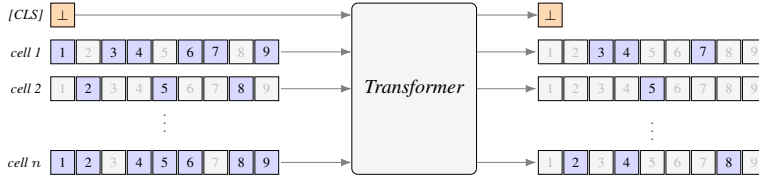


Figure 2: Lattice-tensor encoding in the transformer. Surviving candidates are highlighted; eliminated candidates are greyed. In the output, cell 2 has collapsed to a single candidate.

Recurrent transformer The model is a recurrent transformer closely following Sotaku [11]: a stack of 4 attention layers is unrolled for 16 internal iterations, with the output of iteration ℓ becoming the input to iteration $\ell + 1$. We re-inject the input lattice encoding at every iteration as a residual signal. Each iteration emits its own candidate and conflict logits. At training time every iteration is supervised and contributes equally to the loss; at inference time we read out only the final iteration. Position is encoded with a learned 2D positional embedding added to the input; for the larger 30×30 Maze grids we additionally apply 2D RoPE [30] inside attention.

4.2 Solve Loop and Step Operator

We run the same Solve procedure (Algorithm 1) at training and inference time, which ensures that the distribution of lattice states the model is trained on matches what it encounters at inference. Our setup shares similarities with classical supervised fine-tuning, on-policy distillation [31] and reinforcement learning [32]: as in the latter two, the training distribution is generated by the model’s own rollouts and supervision is state-conditional; as in SFT, the target \hat{y} is computed from data, which we do in a domain-agnostic manner via the abstraction operator α . This gives strong per-step supervision rather than a sparse trajectory-level reward or an approximate teacher signal. The solve loop is a stochastic search that repeatedly applies the step operator, moving down the lattice with deterministic deduction and random branching. This process repeats until a step identifies either a conflict or a solution. Termination is guaranteed because the lattice is finite and each step strictly decreases the alive-candidate count. This outer-loop structure contrasts with recurrent reasoners like TRM [10] and HRM [9], whose outer loop passes a latent embedding between steps; ours passes through the lattice itself. We do not currently propagate gradients across solve steps, though combining the lattice with a TRM/HRM-style cross-step latent is a natural direction for future work.

A single step is summarized in Algorithm 2. We run the recurrent transformer, which unrolls its 16 internal iterations and produces per-candidate confidences at each grid cell and a CLS conflict signal. We then eliminate every candidate whose confidence falls below a threshold θ_{elim} . If the resulting state is neither a complete singleton solution nor flagged inconsistent, we pick a uniformly random multi-candidate cell and pin it to a single digit sampled from a softmax over its alive candidates at

Algorithm 1 Solve (used for both training and inference)

Require: initial lattice state x_0 ; ground-truth solutions Y (empty at inference)

- 1: $x \leftarrow x_0$
 - 2: **repeat**
 - 3: $(x', \text{conflict}, \text{solved}, \mathcal{L}) \leftarrow \text{step}(x, Y)$
 - 4: **if** $Y \neq \emptyset$ **then**
 - 5: Update θ by one optimizer step on \mathcal{L}
 - 6: **end if**
 - 7: $x \leftarrow x'$
 - 8: **until** conflict or solved
 - 9: **return** $x, \text{conflict}, \text{solved}$
-

temperature τ_{decide} . At training time, the conflict and solved flags are verified directly against Y ; at inference time, we trust the model’s CLS prediction and the empty-cell test.

Algorithm 2 Step operator $\text{step}(x, Y)$

Require: lattice state x ; ground-truth solutions Y (empty at inference)

- 1: $(b^{(1..L)}, c^{(1..L)}) \leftarrow f_\theta(x)$ ▷ candidate and CLS logits at every iteration
 - 2: $b \leftarrow b^{(L)}$; $c \leftarrow c^{(L)}$; $\mathcal{L} \leftarrow 0$
 - 3: $x' \leftarrow x$; for every (i, j) with $\sigma(b_{ij}) < \theta_{\text{elim}}$, set $x'_{ij} \leftarrow 0$ ▷ threshold elimination
 - 4: conflict $\leftarrow [\sigma(c) > \theta_{\text{CLS}}]$ or some cell of x' has zero alive candidates
 - 5: solved \leftarrow every cell of x' has exactly one alive candidate **and not** conflict
 - 6: **if** $Y \neq \emptyset$ **then** ▷ in training, use iteration-averaged logits and ground truth
 - 7: $b \leftarrow \frac{1}{L} \sum_{\ell=1}^L b^{(\ell)}$; $c \leftarrow \frac{1}{L} \sum_{\ell=1}^L c^{(\ell)}$
 - 8: $\hat{y} \leftarrow x \cap \alpha(\{y \in Y \mid y \text{ consistent with } x\})$
 - 9: $\mathcal{L} \leftarrow \text{compute_loss}(\hat{y}, b^{(1..L)}, c^{(1..L)})$
 - 10: conflict \leftarrow no $y \in Y$ is consistent with x'
 - 11: solved $\leftarrow x'$ is a singleton matching some $y \in Y$
 - 12: **end if**
 - 13: **if** not conflict and not solved **then** ▷ branch (sample-pin one cell)
 - 14: Pick i^* uniformly at random from cells with ≥ 2 alive candidates
 - 15: Sample $d^* \sim \text{softmax}(b_{i^*} / \tau_{\text{decide}})$ over alive candidates of i^*
 - 16: Pin cell i^* to d^* in x' (zero all other candidates of i^*)
 - 17: **end if**
 - 18: **return** $x', \text{conflict}, \text{solved}, \mathcal{L}$
-

Loss design The candidate-elimination and conflict-detection heads sit at opposite ends of the soundness/completeness trade-off. Candidate elimination must be sound (a wrongly eliminated candidate is unrecoverable) while conflict detection must be complete (a missed conflict can stall search or lead to returning a wrong answer). We supervise every one of the 16 internal iterations with three loss terms: $\mathcal{L}_{\text{BCE}}^{(\ell)}$, an asymmetric BCE between $\sigma(b^{(\ell)})$ and \hat{y} with positive class weight w^+ and negative class weight $w^- < w^+$ to penalize false eliminations more heavily than false retentions; $\mathcal{L}_{\text{CLS}}^{(\ell)}$, a symmetric BCE between $\sigma(c^{(\ell)})$ and $\mathbf{1}[\hat{y} = \perp]$; and $\mathcal{L}_{\text{CE}}^{(\ell)}$, a per-cell softmax cross-entropy on $b^{(\ell)}$ at cells where \hat{y} has a single alive candidate. Adding \mathcal{L}_{CE} helps the model learn faster. The total loss is

$$\mathcal{L} = \frac{1}{L} \sum_{\ell=1}^L \left[\mathcal{L}_{\text{BCE}}^{(\ell)} + \lambda_{\text{cls}} \mathcal{L}_{\text{CLS}}^{(\ell)} + \lambda_{\text{ce}} \mathcal{L}_{\text{CE}}^{(\ell)} \right]. \quad (1)$$

At inference time we eliminate candidates whose probability falls below a threshold θ_{elim} matched to the natural ratio induced by the asymmetric loss; this outperforms training with a symmetric BCE and tuning θ_{elim} post-hoc. When no $y \in Y$ is still consistent with x , the surviving set is empty and \hat{y} collapses to \perp , which would push every candidate sigmoid toward zero and overload the BCE with conflict-detection pressure. The lattice contains many representations of an empty solution set; we pick one that lives further up the lattice by caching the last non-empty \hat{y}^{prev} per chain and using $x \cap \hat{y}^{\text{prev}}$ as the BCE target once the surviving set becomes empty. This keeps the conflict localized to

the individual cells where x has eliminated every candidate alive in \hat{y}^{prev} , focuses the BCE on sound deduction within still-satisfiable cells, and primarily leaves conflict detection to the CLS head (the candidate head can still flag localized conflicts when a cell collapses to empty). In our experiments we use $w^+/w^- = 8$, $\lambda_{\text{cls}} = 0.1$, $\lambda_{\text{ce}} = 0.2$, $\theta_{\text{elim}} \approx 0.1$, and decide temperature $\tau_{\text{decide}} = 1.5$, all tuned on Sudoku and transferred without modification to the other domains we evaluate.

Multi-solution supervision via the α operator Many problems of interest admit a set of solutions rather than a unique answer. Standard supervised fine-tuning, written against a single privileged ground truth, arbitrarily penalizes the model for committing to any of the equally valid alternatives, echoing the insufficiency of using token-level matching (BLEU score) for code generation [33]. We address this, we sample from the full solution space to pre-compute up to K valid solutions $Y = \{y^{(1)}, \dots, y^{(K)}\}$ per puzzle (each a one-hot point on the lattice), drawn uniformly at random from the domain’s solution set (the all-shortest-paths DAG for Maze, the unique solution for Sudoku/Snowflake), and apply the abstraction function α to the subset of Y still consistent with the current state, as in Algorithm 2. As the state commits against solutions, the surviving subset shrinks: at branching cells where two or more solutions still survive, α remains multi-alive, and once the state has committed to a single solution’s path, α collapses to a one-hot. The special case $K = 1$ recovers standard single-target supervised learning. Of our evaluation domains, Sudoku has a unique solution per puzzle ($K = 1$) while the Maze task admits multiple valid paths per instance ($K > 1$); the same procedure handles both. Train-time overhead is minimal: the number of training steps does not depend on K , and K adds only minor bookkeeping per step – in our Maze experiments, $K = 512$ is roughly 2% slower per step than $K = 1$.

Parallel solve Solve describes a single linear chain from the initial state to a terminal, but in practice we parallelize both training and inference. For training, we maintain a pool of recent partially-deduced states, similar to a replay buffer except each instance contributes to a single gradient step. Each batch samples instances from the pool, runs Step, removes those that are truly conflicted or truly solved (verified against Y), and returns the rest to the pool. Over training, the pool develops a natural distribution over lattice depths, giving the model an implicit curriculum of progressively deeper states. At inference, we seed the batch with copies of a single puzzle and step each chain in parallel until one reaches a solution; detected conflicts are replaced by fresh puzzle instances.

Inference tricks (i) Each step is wrapped in a random dataset-level symmetry (a digit permutation composed with a dihedral grid transformation), which we invert after deduction and branching; we omit this augmentation during training, where we found dataset-level augmentation to perform better (the no-aug row of Table 1 uses neither augmentation). (ii) The CLS threshold at inference, $\theta_{\text{CLS}}^{\text{eval}}$, is set slightly higher than at training (we use 0.6 for Sudoku and Snowflake, and 0.53 for the 30×30 Maze-Hard runs). The conflict head grows more confident as the puzzle fills in, so raising the threshold suppresses false-positive conflicts on early-stage states (each of which would reset a deductive chain) while still flagging genuine conflicts at deeper, more committed states; this saves a substantial number of forward passes per solve.

5 Evaluation

5.1 Sudoku-Extreme

We evaluate Lattice Deduction Transformers on Sudoku-Extreme, a benchmark introduced alongside HRM [9]. The puzzles come from the Tdoku puzzle generator and benchmark suite [34], the recurrent-relational-network Sudoku corpus of Palm et al. [35], and the convolutional Sudoku dataset of Park [36]. Puzzles are filtered to retain only instances that require search to solve, as measured by tdoku’s reported guess count per puzzle. This yields puzzles that defeat every known polynomial-time human heuristic and force a non-trivial backtracking depth on symbolic solvers.

We train an 800k parameter Lattice Deduction Transformer on the 1,000 puzzle train set using the procedure described in Section 4.2. Sudoku-Extreme puzzles have unique solutions, so each instance is paired with a single ground-truth solution and the alpha operator reduces to the $K=1$ special case. We augment the training set with the symmetries of Sudoku: any digit permutation and the dihedral group D_4 acting on the grid (rotations and reflections of the 9×9 board). We find that tuning the conflict detection threshold during inference $\theta_{\text{CLS}}^{\text{eval}}$ can slightly improve solver performance by reducing calls and avoiding timeouts; specifically, we use $\theta_{\text{CLS}}^{\text{eval}} = 0.6$, tuned on the train set.

We compare our method to three frontier chain-of-thought LLMs, Claude Opus 4.6 [37], DeepSeek V4-Pro [38] and ChatGPT 5.4 [39]. Additionally, we compare to similar methods in TRM [10] and HRM [9], as well as Sotaku [11]. For the frontier LLMs, we conducted direct zero-shot evaluations. For TRM, HRM and Sotaku, we report the results provided by the respective authors; we did not reproduce their experiments.

Table 1: Test accuracy (%) on Sudoku-Extreme.

Model	Parameters	Train Set	Soundness and Accuracy %	Inference cost	Training Cost
Claude Opus 4.6	?	—	0.0 / 0.0	—	—
DeepSeek V4-Pro	1.6T	—	0.0 / 0.0	—	—
GPT-5.4	?	—	0.0 / 0.0	—	—
HRM	27M	1K	55.0 / 55.0	—	—
TRM	5M	1K	87.4 / 87.4	—	36h (4 × L40S)
Sotaku	800K	2.7M	98.9 / 98.9	—	2h 40m (1 × H100)
LDT, 1K train steps	800K	1K	100 / 85.6	0.78s/ex	4m (1 × B200)
LDT, 2K train steps	800K	1K	100 / 99.3	0.18s/ex	7m (1 × B200)
LDT, 4K train steps	800K	1K	100 / 100	0.028s/ex	15m (1 × B200)
LDT, 4K train steps	800K	1K (no-aug)	100 / 99.7	0.051s/ex	13m (1 × B200)

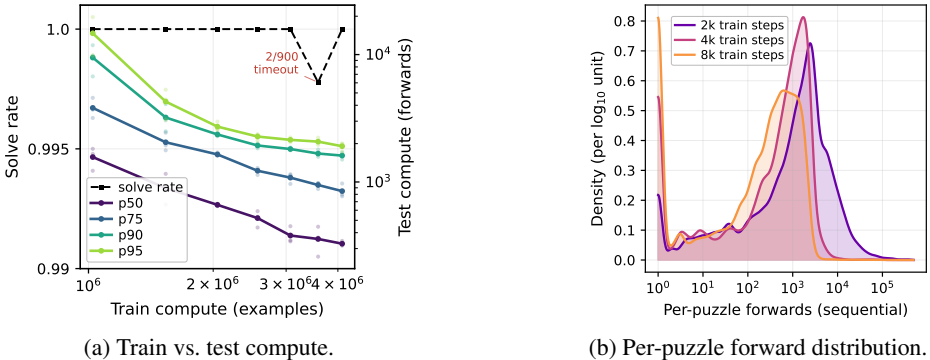


Figure 3: Test/train compute trade-off on Sudoku-Extreme.

Results Table 1 summarizes the performance of the LDT against the other models. Results for HRM, TRM, and Sotaku are as reported in their respective works; frontier LLM results were obtained via our own zero-shot evaluations. Soundness refers to the percentage of responses that are correct or where the method refuses to return a result. Our model reaches empirical soundness around 2K steps and 100% solve rate by 4K, beating the best prior result at a fraction of the training cost; the chain-of-thought LLMs solve no instances. Figure 3a shows the underlying train/test compute trade-off: more training shortens search, with the median and tail percentiles (p50, p75, p90, p95) of per-puzzle forward passes dropping by an order of magnitude as the training budget grows. Across 3 seeds, no run returned a wrong solution; one seed accumulated 2 search timeouts out of 300 puzzles, slightly lowering its solve rate. Figure 3b resolves the underlying distribution: per-puzzle solve times are bimodal, with one mode at puzzles the model solves directly through deduction (no search needed) and a second mode at puzzles that require branching. As training increases, mass shifts from the search mode to the deduction mode and the search-mode peak itself moves to fewer forward passes; better deductions translate to less guessing. TRM relies on data augmentation to stretch the 1K training set; we find augmentation helpful but not required: an LDT trained on the unaugmented 1K puzzles still reaches empirical soundness and 99.7% accuracy by 4K steps (last row of Table 1).

5.2 Snowflake Sudoku

To test whether LDT generalizes beyond the standard 9×9 grid, we evaluate on snowflake Sudoku, a hexagonal variant with variable grid size (Figure 8, Appendix B). A snowflake of order n arranges cells on a hexagonal grid with six triangular arms radiating from a central hub. Each cell takes a

value in $\{1, \dots, 6\}$, and each constraint group (row, arm, or ring) requires all-different values. As n grows from 4 to 8, the number of cells grows from 24 to 48, so the model must handle variable-size puzzles with different constraint patterns.

We generate puzzles using CVC5 [40]: for each order n , CVC5 finds a valid complete assignment, then a greedy minimization pass removes givens while CVC5 verifies that the puzzle retains a unique solution. This yields 1,000 base solutions per order for $n \in \{4, 5, 6, 7, 8\}$ with up to 6 variants each, for roughly 30,000 puzzles in total. We split this pool 90/10 into train and test, then subsample 500 puzzles for training and 1,000 for LDT evaluation; the frontier LLMs are evaluated on a 200-puzzle subsample from the same distribution.

To handle the variable topology with a fixed-size transformer, we embed every puzzle into a fixed 15×10 covering grid that can represent any snowflake topology up to $n = 19$. Each hexagonal cell maps to a deterministic position via axial coordinates (q, r) and triangular direction, with cells absent from a given puzzle zeroed out and excluded from the loss via a per-cell mask. A single model thus handles all puzzle sizes without architecture changes. Training and inference follow the same Solve procedure as Sudoku-Extreme, with the same hyperparameters. Each snowflake puzzle has a unique solution, so α runs at $K = 1$. Full hyperparameters are in Appendix D.1. We use the same baselines as before; TRM, HRM, and Sotaku are not trained on snowflake Sudoku and are omitted.

Table 2: Test accuracy (%) on Snowflake Sudoku.

Model	Parameters	Train Set	Soundness and Accuracy %	Training Cost
Claude Opus 4.6	?	—	0.0 / 0.0	—
DeepSeek V4-Pro	1.6T	—	0.0 / 0.0	—
GPT-5.4	?	—	0.0 / 0.0	—
Lattice Deduction Transformer	800K	500	100 / 100	4m (1× B200)

Table 2 summarizes the performance of the Lattice Deduction Transformer against the chain-of-thought LLMs. Our model solves every test instance with 4 minutes of training on a single B200 GPU, while the chain-of-thought LLMs fail to solve a single instance.

5.3 Maze-Hard

We evaluate Lattice Deduction Transformers on Maze-Hard, a benchmark introduced alongside HRM [9]. The puzzles are 30×30 mazes whose shortest path between start and goal cells has length at least 110. Unlike Sudoku, a single instance can admit millions of distinct shortest paths (Figure 4a), so the alpha operator can run at $K > 1$ by sampling uniformly from the all-shortest-paths DAG.

We follow the same experimental setup as Sudoku-Extreme, with three adjustments for the larger grid: embedding dimension $d = 192$, 2D RoPE positional encodings, and 20,000 training steps at batch size 192. We report two settings, both trained on the 1,000-puzzle Maze-Hard split (matching the TRM setup). The first uses $K = 1$, pairing each instance with a single ground-truth solution; the second uses $K = 512$, sampling 512 shortest paths per instance from the all-shortest-paths DAG.

Table 3: Test accuracy (%) on Maze-Hard.

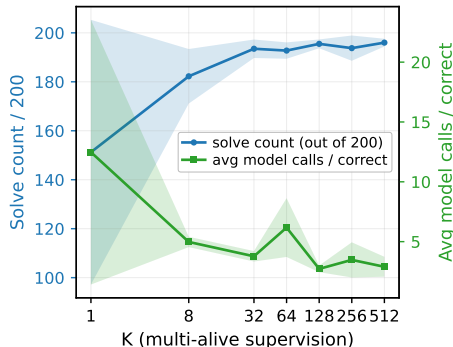
Model	Parameters	Train Set	Soundness and Accuracy %	Training Cost
Claude Opus 4.6	?	—	0.0 / 0.0	—
DeepSeek V4-Pro	1.6T	—	0.0 / 0.0	—
GPT-5.4	?	—	0.0 / 0.0	—
HRM	27M	1K	74.5 / 74.5	—
TRM	7M	1K	85.3 / 85.3	24h (4× L40S)
LDT, $K = 1$	1.8M	1K	99.3 / 99.3	9.7h (1× B200)
LDT, $K = 512$	1.8M	1K	99.9 / 99.9	9.8h (1× B200)

Table 3 reports two settings, both trained on the 1,000-puzzle Maze-Hard split. With $K = 1$, LDT solves 993/1000 test instances; with $K = 512$, it solves 999/1000. Neither is empirically sound: the unsolved instances emitted incorrect solutions rather than abstaining. The incorrect solutions are nonetheless valid paths from start to goal, just of slightly suboptimal length.

Multi-solution supervision via α A typical 30×30 maze admits millions of distinct shortest paths, so $K = 512$ samples only a small fraction of the valid solution set. The Solve loop’s per-step target is $\hat{y} = x \sqcap \alpha(\{y \in Y \mid y \text{ consistent with } x\})$, so as K grows we feed the model an increasingly informative intersection of valid solutions and the supervision signal sharpens without changing the architecture or loss. Figure 4b plots solve rate and batched forward passes per puzzle as a function of K ; larger K yields a strictly tighter target, a higher solve rate, and shorter searches at inference. The gain is concentrated at small K and saturates quickly: most of the benefit is recovered with a handful of sampled solutions, and further increases yield diminishing returns. Tasks with different solution-set geometry may show different curves.



(a) Maze-Hard example (30×30).



(b) Solve rate and batched forwards vs. K .

Figure 4: Maze-Hard task and multi-solution supervision via α . (a) one 30×30 Maze-Hard instance with start, goal, and several of the many shortest paths of equal length. (b) solve rate and batched forward passes per puzzle as a function of the sample budget K , averaged over 4 seeds on 15×15 grids with minimum shortest-path length 27, trained for 4,000 steps.

6 Conclusion

We introduced the Lattice Deduction Transformer (LDT), an architecture analogous to diffusion that iteratively refines a solution through forward passes capturing sound step-by-step deduction, rather than opaque latent updates. The model is trained via the Solve procedure on a batch of partially-deduced lattice states that evolves under its own forward pass and supervised against the alpha operator. At inference, a parallel solve runs many chains per puzzle through the same deduction operator and exploits its soundness to either return a correct answer or abstain. Together, this allows an 800,000-parameter model to match or exceed frontier-LLM performance on hard reasoning benchmarks while remaining empirically sound. More broadly, the iterative-refinement structure LDT shares with diffusion suggests a productive interface for borrowing techniques across the two literatures. While we instantiate LDT on combinatorial puzzles, the architecture is agnostic to the underlying lattice; any abstract domain admitting a deduction operator could in principle be substituted.

Limitations LDT is well-suited to tasks with clear logical structure, where a fixed set of rules induces a sound deduction operator that the model learns to apply. Benchmarks like ARC-AGI [41, 42, 43] demand something stronger: each task carries its own rules, which the model must *infer* from a handful of demonstrations before it can deduce anything about the test input. A naive port of LDT plateaus at roughly 36% pass rate, with no gains from test-time search – the conflict head becomes unreliable, so the search cannot tell good branches from bad. Closing this gap will likely require additional machinery from TRM [10], in particular deep supervision that pushes a useful gradient through every intermediate lattice state and stronger recursive structure across deduction steps in place of simple iteration. More speculatively, this setting may require a different abstract domain entirely: one over the *programs* that produce solutions, rather than over the solution states themselves.

References

- [1] Jason Wei, Xuezhi Wang, Dale Schuurmans, Maarten Bosma, Brian Ichter, Fei Xia, Ed Chi, Quoc Le, and Denny Zhou. Chain-of-thought prompting elicits reasoning in large language models. In *Advances in Neural Information Processing Systems*, volume 35, 2022.
- [2] Xuezhi Wang, Jason Wei, Dale Schuurmans, Quoc Le, Ed H. Chi, Sharan Narang, Aakanksha Chowdhery, and Denny Zhou. Self-consistency improves chain of thought reasoning in language models. In *International Conference on Learning Representations (ICLR)*, 2023.
- [3] Charlie Snell, Jaehoon Lee, Kelvin Xu, and Aviral Kumar. Scaling LLM test-time compute optimally can be more effective than scaling parameters for reasoning. In *International Conference on Learning Representations (ICLR)*, 2025.
- [4] Jacob Austin, Daniel D. Johnson, Jonathan Ho, Daniel Tarlow, and Rianne van den Berg. Structured denoising diffusion models in discrete state-spaces. In *Advances in Neural Information Processing Systems (NeurIPS)*, 2021.
- [5] P. Cousot and R. Cousot. Abstract interpretation: a unified lattice model for static analysis of programs by construction or approximation of fixpoints. In *Conference Record of the Fourth Annual ACM SIGPLAN-SIGACT Symposium on Principles of Programming Languages*, pages 238–252, Los Angeles, California, 1977. ACM Press, New York, NY.
- [6] P. Cousot and R. Cousot. Systematic design of program analysis frameworks. In *Conference Record of the Sixth Annual ACM Symposium on Principles of Programming Languages*, pages 269–282, San Antonio, Texas, 1979. ACM Press, New York, NY.
- [7] Alex Graves. Adaptive computation time for recurrent neural networks, 2016.
- [8] Mostafa Dehghani, Stephan Gouws, Oriol Vinyals, Jakob Uszkoreit, and Łukasz Kaiser. Universal transformers. In *International Conference on Learning Representations (ICLR)*, 2019.
- [9] Guan Wang, Jin Li, Yuhao Sun, Xing Chen, Changling Liu, Yue Wu, Meng Lu, Sen Song, and Yasin Abbasi Yadkori. Hierarchical reasoning model, 2025.
- [10] Alexia Jolicoeur-Martineau. Less is more: Recursive reasoning with tiny networks, 2025.
- [11] Cheng Lou. Sotaku: From-scratch experiments on iterative neural Sudoku solvers. Software, GitHub repository <https://github.com/chenglou/sotaku>, commit 9e13341, 2026. Accessed: 2026-05-07.
- [12] Po-Wei Wang, Priya L. Donti, Bryan Wilder, and J. Zico Kolter. SATNet: Bridging deep learning and logical reasoning using a differentiable satisfiability solver. In *Proceedings of the 36th International Conference on Machine Learning (ICML)*, volume 97 of *Proceedings of Machine Learning Research*, pages 6545–6554. PMLR, 2019.
- [13] Matt Fredrikson, Kaiji Lu, Saranya Vijayakumar, Somesh Jha, Vijay Ganesh, and Zifan Wang. Learning modulo theories. *arXiv preprint arXiv:2301.11435*, 2023.
- [14] Shaurya Gumber and Gagandeep Singh. Neural abstract interpretation. In *ICLR 2025 Workshop: VerifAI: AI Verification in the Wild*, 2025.
- [15] Jingxuan He, Gagandeep Singh, Markus Püschel, and Martin Vechev. Learning fast and precise numerical analysis. In *Proceedings of the 41st ACM SIGPLAN Conference on Programming Language Design and Implementation (PLDI)*, pages 1112–1127, 2020.
- [16] Qiuhan Gu, Avaljot Singh, and Gagandeep Singh. SAIL: Sound abstract interpreters with LLMs. *Proceedings of the ACM on Programming Languages*, 10(PLDI), 2026. To appear.
- [17] Gagandeep Singh, Markus Püschel, and Martin Vechev. Fast numerical program analysis with reinforcement learning. In *Computer Aided Verification (CAV)*, volume 10981 of *Lecture Notes in Computer Science*, pages 211–229. Springer, 2018.

- [18] Sooyoung Cha, Sehun Jeong, and Hakjoo Oh. Learning a strategy for choosing widening thresholds from a large codebase. In *Programming Languages and Systems (APLAS)*, volume 10017 of *Lecture Notes in Computer Science*, pages 25–41. Springer, 2016.
- [19] Jacob Devlin, Ming-Wei Chang, Kenton Lee, and Kristina Toutanova. BERT: Pre-training of deep bidirectional transformers for language understanding. In *Proceedings of the 2019 Conference of the North American Chapter of the Association for Computational Linguistics: Human Language Technologies (NAACL-HLT)*, pages 4171–4186, 2019.
- [20] Guanghan Wang, Yair Schiff, Subham Sekhar Sahoo, and Volodymyr Kuleshov. Remasking discrete diffusion models with inference-time scaling. In *Advances in Neural Information Processing Systems (NeurIPS)*, 2025.
- [21] Chen-Hao Chao, Wei-Fang Sun, Hanwen Liang, Chun-Yi Lee, and Rahul G. Krishnan. Beyond masked and unmasked: Discrete diffusion models via partial masking. In *Advances in Neural Information Processing Systems (NeurIPS)*, 2025.
- [22] Cai Zhou, Chenyu Wang, Dinghuai Zhang, Shangyuan Tong, Yifei Wang, Stephen Bates, and Tommi Jaakkola. Next semantic scale prediction via hierarchical diffusion language models. In *Advances in Neural Information Processing Systems (NeurIPS)*, 2025.
- [23] Martin Davis and Hilary Putnam. A computing procedure for quantification theory. *Journal of the ACM*, 7(3):201–215, 1960.
- [24] Martin Davis, George Logemann, and Donald Loveland. A machine program for theorem-proving. *Communications of the ACM*, 5(7):394–397, 1962.
- [25] João P. Marques-Silva, Inês Lynce, and Sharad Malik. Conflict-driven clause learning SAT solvers. In Armin Biere, Marijn Heule, Hans van Maaren, and Toby Walsh, editors, *Handbook of Satisfiability*, volume 185 of *Frontiers in Artificial Intelligence and Applications*, pages 131–153. IOS Press, 2009.
- [26] Mary Sheeran and Gunnar Stålmarck. A tutorial on stålmarck’s proof procedure for propositional logic. In Ganesh Gopalakrishnan and Phillip Windley, editors, *Formal Methods in Computer-Aided Design*, pages 82–99, Berlin, Heidelberg, 1998. Springer Berlin Heidelberg.
- [27] Sergei Leonov and Liam Davis. Two optimizations on the stålmarck procedure, 2025.
- [28] Vijay D’Silva, Leopold Haller, and Daniel Kroening. Abstract conflict driven learning. In *Proceedings of the 40th Annual ACM SIGPLAN-SIGACT Symposium on Principles of Programming Languages (POPL)*, pages 143–154. ACM, 2013.
- [29] Aditya V. Thakur and Thomas W. Reps. A generalization of stålmarck’s method. In *Static Analysis – 19th International Symposium (SAS)*, volume 7460 of *Lecture Notes in Computer Science*, pages 334–351. Springer, 2012.
- [30] Jianlin Su, Murtadha Ahmed, Yu Lu, Shengfeng Pan, Wen Bo, and Yunfeng Liu. RoFormer: Enhanced transformer with rotary position embedding. *Neurocomputing*, 568:127063, 2024.
- [31] Rishabh Agarwal, Nino Vieillard, Yongchao Zhou, Piotr Stanczyk, Sabela Ramos, Matthieu Geist, and Olivier Bachem. On-policy distillation of language models: Learning from self-generated mistakes. In *International Conference on Learning Representations (ICLR)*, 2024.
- [32] Richard S. Sutton and Andrew G. Barto. *Reinforcement Learning: An Introduction*. MIT Press, 2 edition, 2018.
- [33] Shuo Ren, Daya Guo, Shuai Lu, Long Zhou, Shujie Liu, Duyu Tang, Neel Sundaresan, Ming Zhou, Ambrosio Blanco, and Shuai Ma. Codebleu: a method for automatic evaluation of code synthesis, 2020.
- [34] Tom Dillon. Tdoku: A fast Sudoku solver and generator. Software, GitHub repository <https://github.com/t-dillon/tdoku>, 2025. Accessed: 2026-04-27.
- [35] Rasmus Berg Palm, Ulrich Paquet, and Ole Winther. Recurrent relational networks. In *Advances in Neural Information Processing Systems (NeurIPS)*, volume 31, 2018.

- [36] Kyubyong Park. Can convolutional neural networks crack Sudoku puzzles? Software, GitHub repository <https://github.com/Kyubyong/sudoku>, 2018. Accessed: 2026-05-07.
- [37] Anthropic. Introducing claude opus 4.6. Anthropic News, February 2026. Accessed: 2026-04-29.
- [38] DeepSeek-AI. Deepseek-v4 preview release: Ushering in the era of 1m context length. DeepSeek Official Blog, April 2026. Accessed: 2026-04-29.
- [39] OpenAI. Gpt-5.4 thinking system card. Technical report, OpenAI, March 2026.
- [40] Haniel Barbosa, Clark W. Barrett, Martin Brain, Gereon Kremer, Hanna Lachnitt, Makai Mann, Abdalrhman Mohamed, Mudathir Mohamed, Aina Niemetz, Andres Nötzli, Alex Ozdemir, Mathias Preiner, Andrew Reynolds, Ying Sheng, Cesare Tinelli, and Yoni Zohar. cvc5: A versatile and industrial-strength SMT solver. In Dana Fisman and Grigore Rosu, editors, *Tools and Algorithms for the Construction and Analysis of Systems - 28th International Conference, TACAS 2022, Held as Part of the European Joint Conferences on Theory and Practice of Software, ETAPS 2022, Munich, Germany, April 2-7, 2022, Proceedings, Part I*, Lecture Notes in Computer Science, pages 415–442. Springer, 2022.
- [41] François Chollet. On the measure of intelligence. *arXiv preprint arXiv:1911.01547*, 2019.
- [42] Francois Chollet, Mike Knoop, Gregory Kamradt, Bryan Landers, and Henry Pinkard. Arc-agi-2: A new challenge for frontier ai reasoning systems, 2025.
- [43] ARC Prize Foundation. Arc-agi-3: A new challenge for frontier agentic intelligence, 2026.

A Abstract Interpretation for Logical Problems

This appendix gives a formal introduction to abstract interpretation. The framework is most often presented in the setting of program analysis, where the concrete domain is the (typically infinite) set of program states; here we sketch the simpler instance that suffices for our purposes, in which the concrete domain captures candidate solutions to a finite-domain logical problem such as Sudoku.

A.1 Lattices and Galois Connections

A *lattice* $(L, \sqsubseteq, \sqcup, \sqcap)$ is a set L equipped with a partial order \sqsubseteq in which every pair $a, b \in L$ has a least upper bound $a \sqcup b$ (the *join*) and a greatest lower bound $a \sqcap b$ (the *meet*). A lattice is *bounded* if it has a top element \top above every element and a bottom element \perp below every element. Following the main text, we read \sqsubseteq as a precision ordering: $a \sqsubseteq b$ means a is at least as informative as b , with \perp inconsistent and \top uninformative.

Recall that a Sudoku solution is a function $g : \{1, \dots, 9\}^2 \rightarrow \{1, \dots, 9\}$, and write G for the set of all such grids. We construct two lattices over G .

Our *concrete domain* is the *powerset lattice* $C = (2^G, \subseteq, \cup, \cap)$ over G , with $\perp = \emptyset$ and $\top = G$. An element of C is the set of complete grids still considered viable; smaller sets carry more information about which grid is correct and therefore sit lower in the lattice.

The *grid powerset lattice* is the per-cell pointwise version, $A = (\{1, \dots, 9\}^2 \rightarrow 2^{\{1, \dots, 9\}})$, ordered by $a \sqsubseteq b$ iff $a(c) \subseteq b(c)$ for every cell c . Meet is pointwise intersection, join is pointwise union, \top is the constant map sending every cell to $\{1, \dots, 9\}$, and \perp is identified with any map having an empty candidate set at some cell. An element of A records, for each cell, which digits are still considered viable for that cell. By construction, the grid powerset lattice loses all relational information across cells: any correlation between distinct cell values present in a concrete state is forgotten when only per-cell candidate sets are tracked.

An abstract element $a \in A$ can be read as the set of complete grids that respect its candidate sets. We make this precise with the *concretization* map $\gamma : A \rightarrow C$,

$$\gamma(a) = \{g \in G : g(c) \in a(c) \text{ for every cell } c\}.$$

Concretization is monotone: $a \sqsubseteq b$ implies $\gamma(a) \subseteq \gamma(b)$.

Conversely, given $S \in C$ we look for the most informative abstract element whose concretization still covers S — that is, $S \subseteq \gamma(a)$, so that abstracting away does not discard any candidate in S . The *abstraction* map $\alpha : C \rightarrow A$ returns this best sound approximation, given elementwise by

$$\alpha(S)(c) = \{g(c) : g \in S\},$$

the set of digits assigned to cell c by some grid in S . The pair (α, γ) forms a *Galois connection*, written in the standard notation

$$C \begin{array}{c} \xrightarrow{\alpha} \\ \xleftarrow{\gamma} \end{array} A.$$

Here α is the *lower adjoint* (the upper, rightward arrow) and γ is the *upper adjoint* (the lower, leftward arrow). The two arrows encode two round-trip conditions, each obtained by tracing a path from one side back to itself:

$$S \subseteq \gamma(\alpha(S))$$

$$\alpha(\gamma(a)) \sqsubseteq a.$$

We use \subseteq for the concrete order on C and \sqsubseteq for the abstract order on A . The first condition says that going to the abstract domain and back can only *add* candidates to the original solution set: abstraction is sound because the round trip overapproximates. The second is more intuitive: going to the concrete and back lets us *refine* the abstract representation by stripping out structure that no concrete element witnesses. Figures 5 and 6 illustrate the two directions on 2×2 Sudoku puzzles.

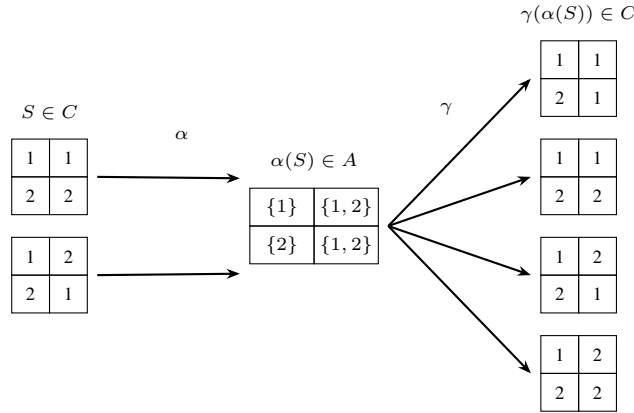


Figure 5: Round-trip $\gamma \circ \alpha$ on 2×2 Sudoku. The set S contains two grids that differ in the right-hand column. Abstraction drops the cell-to-cell correlation, so concretizing the result yields four grids — the original two plus two additional grids that satisfy the per-cell candidate sets but were not in S .

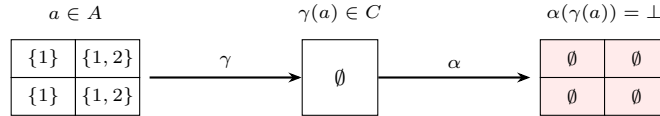


Figure 6: Round-trip $\alpha \circ \gamma$ on an impossible abstract element. Column 1 of a forces both rows to take the value 1, contradicting the column constraint, so $\gamma(a) = \emptyset$. Re-abstrating then collapses every cell to the empty candidate set, refining a all the way to \perp .

A.2 Sound Function Approximation and Deduction

Abstract interpretation is usually concerned not with single states but with *operations* on states — for instance, the function that takes a program point to its successor state. We are therefore interested in approximating monotone functions $f : L \rightarrow L$ on a lattice. In the abstract interpretation literature these are called *transformers*; we avoid that term to prevent confusion with the transformer neural architecture, and simply refer to monotone functions on L .

The intuition for monotonicity is that the function is applied uniformly to every member of a state of knowledge: if a is at least as informative as b , then $f(a)$ is at least as informative as $f(b)$, because strengthening the input can only produce a more committed output.

Given lattices L_1 and L_2 , the monotone functions $L_1 \rightarrow L_2$ themselves form a lattice under the pointwise order: $f \sqsubseteq g$ iff $f(x) \sqsubseteq g(x)$ for every x . A Galois connection $C \xrightleftharpoons[\gamma]{\alpha} A$ on point lattices lifts to a Galois connection between the function lattices $[C \rightarrow C]$ and $[A \rightarrow A]$, with abstraction $\alpha^\sharp(f) = \alpha \circ f \circ \gamma$ and concretization $\gamma^\sharp(f^\sharp) = \gamma \circ f^\sharp \circ \alpha$. Figure 7 sketches the construction.

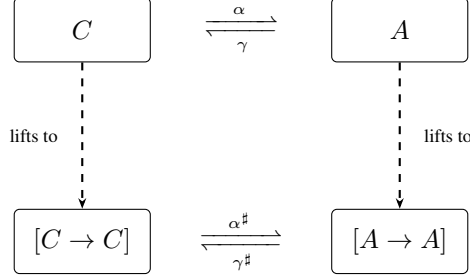


Figure 7: Lifting a Galois connection to monotone-function lattices. The Galois connection between the point lattices C and A induces a Galois connection between the corresponding lattices of monotone functions, with $\alpha^\sharp(f) = \alpha \circ f \circ \gamma$ and $\gamma^\sharp(f^\sharp) = \gamma \circ f^\sharp \circ \alpha$.

For a concrete monotone function f , the lifted abstraction $\alpha^\sharp(f) = \alpha \circ f \circ \gamma$ is the most precise sound approximation of f on A (traditionally called the *best abstract transformer*). It is typically intractable to compute directly, so in practice one works with a weaker abstract function f^\sharp that is still sound, meaning $\alpha \circ f \circ \gamma \sqsubseteq f^\sharp$.

The result that justifies all of this is that fixed points transfer [5, 6]: if f is monotone on C and f^\sharp is any sound abstraction, then

$$\alpha(\text{lfp } f) \sqsubseteq \text{lfp } f^\sharp \quad \text{and} \quad \alpha(\text{gfp } f) \sqsubseteq \text{gfp } f^\sharp.$$

Computing a fixed point in the abstract domain therefore yields a sound overapproximation of the corresponding fixed point in the concrete.

Logical problems and deduction In a logical problem the goal is solution-finding rather than the analysis of a dynamic system over time. The function of interest is the *deduction function* of the puzzle ϕ ,

$$\text{ded}_\phi : C \rightarrow C, \quad \text{ded}_\phi(S) = \{g \in S : g \text{ satisfies } \phi\},$$

which filters a candidate set down to those grids that respect the constraints imposed by ϕ . (The function ded_ϕ is a *lower closure operator*: monotone, reductive $\text{ded}_\phi(S) \subseteq S$, and idempotent.) The same pattern applies to any logic L whose formulas are interpreted over a set of models: ded_ϕ keeps only the models of ϕ .

The greatest fixed point of ded_ϕ from $\top = G$ is the set of all solutions to ϕ , and a single application of the best abstract transformer $\alpha \circ \text{ded}_\phi \circ \gamma$ would solve the puzzle in one shot. Practical deduction rules – naked singles, hidden singles, naked pairs, X-wings, and so on – are sound but weaker abstract approximations of ded_ϕ : each removes only some of the candidates the full filter would. Solving a Sudoku then amounts to computing the greatest fixed point of an abstract deduction function in the grid powerset lattice, starting from \top and descending until no further candidates can be removed. Depending on the strength of the chosen rules, the fixed point is either a fully determined grid (the puzzle is solved) or one that leaves multiple candidates open in some cells, in which case search must be invoked to finish the job.

A dual function of interest is the *abduction function* $\text{abd}_\phi : C \rightarrow C$, which extends a candidate set by adding all grids that fail to satisfy ϕ :

$$\text{abd}_\phi(S) = S \cup \{g \in G : g \not\models \phi\}.$$

Where deduction lives in the over-approximation regime we have discussed so far – abstract states bound the true answer from above – abduction lives in the dual under-approximation regime: an

underapproximation of abd_ϕ identifies a region of the search space whose elements are all guaranteed failures. This is the engine of conflict analysis in modern SAT solvers [25]: on a failed search branch, the solver generalizes the witnessed failure into a learned clause that excludes a much larger region than just the assignment that failed, and this adaptive search-space compression (clause learning) is the core reason for the extraordinary performance of modern SAT solvers. The clause-learning step can itself be cast as an abstract interpretation [28]. One motivation for this work is to begin closing the gap between diffusion-style sampling procedures and the advanced search techniques developed in the automated reasoning community.

A note for readers familiar with program analysis The shape of this setup may look unfamiliar to readers fluent in abstract interpretation as it is usually presented. Classically one computes a *least* fixed point over a monotone function encoding program semantics – typically the strongest-postcondition transformer forward, or the weakest-precondition transformer backward. Here we instead compute a *greatest* fixed point over an approximation of a lower closure operator. The difference is purely conventional and historical: abstract interpretation is fundamentally a theory of sound approximation and representation in inferential computation, and the program-semantics framing is one application among several. Logical deduction, constraint satisfaction, and the puzzle setting we use here all fall comfortably within the same theory.

B Snowflake Sudoku Diagram

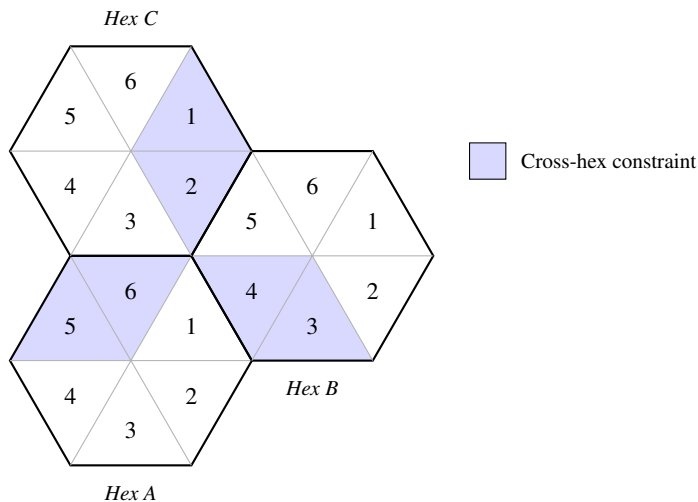


Figure 8: A snowflake Sudoku with $n = 3$ (3 hexagons, 18 cells). Each hexagon is divided into 6 triangular cells, each taking a value in $\{1, \dots, 6\}$. Intra-hex constraints require all 6 cells within each hexagon to be distinct. The shaded cells form a cross-hex constraint group: 2 cells from each hexagon that must also be mutually distinct.

C LLM Baseline Prompts

C.1 Sudoku-Extreme

System prompt

```
You are a Sudoku solver. You will be given a 9 × 9 Sudoku puzzle.
Solve it and respond ONLY with the completed 9 × 9 grid, one row per
line, digits only, no spaces or other characters. Example response
format:
534678912
672195348
...
345286179
```

User prompt

```
Solve this Sudoku:
{puzzle_text}
({puzzle_text} is the puzzle as 9 lines of 9 characters each, with
empty cells written as 0.)
```

C.2 Snowflake Sudoku

System prompt

```
You are solving a Snowflake Sudoku puzzle, a Sudoku variant played
on a snowflake-shaped topology of  $N$  cells, each holding a digit
from 1 to 6. The puzzle is defined by a list of constraint groups;
each group is a set of cell IDs whose digits must all be distinct.
You will be given (1) the total number of cells, (2) the list of
constraint groups, and (3) the current cell values, where ? marks
a cell you must solve and an integer 1-6 marks a given. Respond
with ONLY the solution: one line per cell in order, formatted
as CELL_ID:DIGIT with no spaces, comments, or other text. Output
exactly  $N$  lines. Example:
```

```
0:3
1:5
2:1
3:6
4:2
5:4
```

User prompt

```
Solve this Snowflake Sudoku:
{puzzle_text}
({puzzle_text} encodes the puzzle size, the constraint topology, and
the current cell values, e.g.):
Puzzle (n=4, 24 cells):
Constraint groups (each group must contain distinct digits):
  Group 0: [0, 1, 2, 3, 4, 5]
  Group 1: [6, 7, 8, 9, 10, 11]
  Group 2: [12, 13, 14, 15, 16, 17]
  ...
Cell values (? = solve this):
  Cell 0: 3
  Cell 1: ?
  Cell 2: ?
  Cell 3: 6
  ...
```

C.3 Maze-Hard

System prompt

```
You are a maze solver. You will be given a  $30 \times 30$  maze. Every cell
of the maze is exactly one of the following four characters:
```

```
'#' - wall (impassable)
' ' - free cell
'S' - the start cell (exactly one)
'G' - the goal cell (exactly one)
```

```
Find a path of orthogonally adjacent (up/down/left/right) free cells
that connects S to G without passing through any wall. Diagonal
moves are not allowed. Mark every free cell that lies on the path
with the character o. The cells #, S, and G are unchanged, and free
```

cells that are not on the path remain ' '. Respond with ONLY the completed 30×30 grid: exactly 30 lines, each containing exactly 30 characters drawn from the set $\{\#, ' ', S, G, o\}$. Do not include row numbers, column markers, blank lines, code fences, prose, or any other text. Whitespace inside each row is significant: a leading or trailing space is itself a free cell, not formatting. Example response format (shown for a 6×6 maze for brevity; your output must be 30 rows of 30 characters):

```
#####
#Sooo#
# #o#
# #o#
## ooG
#####
```

User prompt

```
Solve this maze:
{puzzle_text}
({puzzle_text} is the maze as 30 lines of 30 characters each, drawn
from  $\{\#, ' ', S, G\}$ .)
```

D Hyperparameters

D.1 Base set (Sudoku-Extreme and Snowflake)

The base set is used for both Sudoku-Extreme (Section 5.1) and Snowflake Sudoku (Section 5.2).

Architecture Looped transformer with embedding dimension $d = 128$, 4 layers, 4 attention heads, $L = 16$ internal loops per forward pass, FFN multiplier 4.0, dropout $p = 0.1$ during training. Total parameter count is $\approx 800,000$. Sudoku-Extreme uses 9 input channels per cell, one candidate sigmoid per digit. Snowflake Sudoku uses 7 channels per cell (6 candidate sigmoids plus a read-only *in-puzzle* mask channel that the deduction operator leaves untouched), embedded in a fixed 15×10 covering grid that admits every snowflake topology up to order $n = 19$ via deterministic (q, r) axial coordinates and a triangular direction.

Optimizer AdamW with learning rate 3×10^{-3} , weight decay 0.1, $\beta = (0.9, 0.95)$, gradient clip 1.0, cosine schedule with a linear warmup over the first 10% of total training steps.

Solve-procedure training Batch size $B = 512$ with pool-to-batch multiplier 1 (the pool holds exactly one batch and all of it is consumed per step, so the configuration is equivalent to not having a pool). Sudoku-Extreme is trained for $T = 4,000$ steps over the 1,000-puzzle train split ($\approx 2,048$ epochs; $T \in \{1,000, 2,000\}$ also reported in Table 1, at ≈ 512 and $\approx 1,024$ epochs respectively). Snowflake is trained for $T = 1,000$ steps over 500 puzzles ($\approx 1,024$ epochs). Maximum pool age $\tau_{\text{age}} = 100$ training steps since insertion. Augmentation is applied only at the dataset level: each puzzle is wrapped in a random digit-permutation composed with a dihedral grid symmetry before it enters the training pool. We do not use per-step augmentation during training; we tried it and found it to hurt. The Sudoku-Extreme runs reported in Table 1 (other than the no-aug row) and the Snowflake-Sudoku run all use this dataset-level augmentation; for Snowflake the dihedral component is disabled because the square group does not preserve the hex topology of in-puzzle cells. Random seed 0.

No-augmentation variant The no-aug row of Table 1 drops both augmentation channels: training sees only the raw 1,000-puzzle Sudoku-Extreme split with no dataset-level expansion, and inference is run without the per-step symmetry wrapping below. All other hyperparameters match the base set.

Loss weights BCE class weights $w^+ = 4.0$ on positive candidates and $w^- = 0.5$ on negatives; auxiliary softmax cross-entropy weight $\lambda_{\text{ce}} = 0.2$; CLS BCE weight $\lambda_{\text{cls}} = 0.1$.

Inference defaults (Section 4.2) At inference we batch the parallel solve along two axes. A *slot* holds one puzzle from the moment it enters the batch until that puzzle either self-accepts (a chain reaches a complete, operator-accepted solution) or hits the per-puzzle round budget; we run $M = 8$ slots concurrently, evicting and refilling slots from a queue of remaining test puzzles. Within each slot, $K = 64$ *chains* explore the same starting state in parallel but diverge under the stochastic decide (singleton-branching) picks and per-step augmentations – effectively K independent restarts of the search for the same puzzle. One forward pass therefore spans $M \cdot K = 512$ rows. Per-puzzle round budget $R = 1,000$, decide temperature $\tau_{\text{decide}} = 1.5$, eval-time dropout $p_{\text{drop}} = 0.05$, conflict threshold $\theta_{\text{CLS}}^{\text{eval}} = 0.6$, tuned on the Sudoku-Extreme train set. We additionally apply *per-step augmentation* at inference: at each Solve step the lattice state is wrapped in a fresh random digit-permutation composed with a dihedral symmetry, the model performs deduction and branching in that augmented frame, and we invert the symmetry before writing back to the canonical state. This decorrelates the parallel chains and broadens the inference search. We tried mirroring it during training and found it hurt; our working explanation is that training benefits from concentrating gradient on a single canonical Solve trajectory per puzzle, whereas noising every step diffuses that signal across symmetry-equivalent states.

Sequential-cost estimation Figure 3b reports per-puzzle forward-pass counts as a sequential (batch-1) search would have paid, even though inference is run with the parallel slot/chain batch described above. We index the K chains within a slot in ascending order $0, 1, \dots, K - 1$ and admit a fresh puzzle to a slot whenever the current one terminates. For each puzzle, let chain w be the first to reach an accepted solution at round d_w . The sequential cost we report is $\sum_{c < w} \ell_c + d_w$, where ℓ_c is the round at which chain c would have self-terminated (by conflict or its own solution) on its own. To recover ℓ_c exactly for $c < w$, we *drain* the slot after the winner: chains $0, \dots, w - 1$ are left running on the same puzzle until each one terminates, recording its own ℓ_c . This yields precise sequential-cost estimates without re-running the solve at batch 1.

D.2 Maze

For Maze (Section 5.3) we keep the base set above except for the following changes.

General Embedding dimension $d = 192$ (vs. 128; $\approx 1.8\text{M}$ parameters total). Augmentation is dihedral only – digit-permutation is disabled because the channels (wall, free, start, goal, path) carry distinct semantics.

15 × 15 setting Used for the multi-solution supervision sweep (Figure 4b). Batch size $B = 256$, total training steps $T = 4,000$ (≈ 102 epochs over a 10,000-puzzle synthetic training set), inference conflict threshold $\theta_{\text{CLS}}^{\text{eval}} = 0.6$ (matching the base set), K swept across runs. Each K value is averaged over 4 random seeds; for every seed we procedurally generate a fresh 10,000-puzzle training set from the same distribution (the seed controls both the data and the optimizer).

30 × 30 setting Used for the headline Maze-Hard results (Table 3). 2D RoPE added inside attention on top of the base set’s learned 2D positional embedding. Batch size $B = 192$, total training steps $T = 20,000$, pool-to-batch multiplier 2.0, eval-time dropout $p_{\text{drop}} = 0$ (vs. 0.05 elsewhere), inference conflict threshold $\theta_{\text{CLS}}^{\text{eval}} = 0.53$, calibrated on a held-out Maze-Hard set. We report two K configurations, both trained on the 1,000-puzzle Maze-Hard split for $T = 20,000$ steps ($\approx 3,840$ epochs): $K = 1$ (head-to-head with TRM) and $K = 512$.